

## New Limit on the Decay $\mu^+ \rightarrow e^+ \gamma$

P. Depommier, J.-P. Martin, J.-M. Poutissou, and R. Poutissou

*Laboratoire de Physique Nucléaire, Université de Montréal, Montréal, Québec H3C 3J7, Canada*

and

D. Berghofer, M. D. Hasinoff, D. F. Measday, and M. Salomon

*Physics Department, University of British Columbia, Vancouver, British Columbia V6T 1W5, Canada*

and

D. Bryman

*TRIUMF, University of British Columbia, Vancouver, British Columbia V6T 1W5, Canada*

and

M. Dixit and J. A. Macdonald

*Physics Department—TRIUMF, University of Victoria, Victoria, British Columbia V8W 2Y2, Canada*

and

G. I. Opat<sup>(a)</sup>

*School of Physics, University of Melbourne, Parkville, Victoria 3052, Australia*

(Received 16 August 1977)

Using two large NaI detectors, a limit on the branching ratio for the  $\mu^+ \rightarrow e^+ \gamma$  decay has been found to be  $R_{\mu e \gamma} = \Gamma(\mu^+ \rightarrow e^+ \gamma) / \Gamma(\mu^+ \rightarrow e^+ \nu_e \bar{\nu}_\mu) < 3.6 \times 10^{-9}$  at a 90% confidence level.

Evidence for the conservation of muon number rests primarily on the absence of the processes  $\mu^+ \rightarrow e^+ \gamma$ ,<sup>1</sup>  $\mu^+ \rightarrow e^+ e^+ e^-$ ,<sup>2</sup> and  $\mu^- + N \rightarrow e^- + N$ .<sup>3</sup> The present limits (90% confidence level) on these reactions are

$$R_{\mu^+ \rightarrow e^+ \gamma} = \frac{\Gamma(\mu^+ \rightarrow e^+ \gamma)}{\Gamma(\mu^+ \rightarrow e^+ \nu_e \bar{\nu}_\mu)} < 2.2 \times 10^{-8}, \quad (1)$$

$$R_{\mu^+ \rightarrow e^+ e^+ e^-} = \frac{\Gamma(\mu^+ \rightarrow e^+ e^+ e^-)}{\Gamma(\mu^+ \rightarrow e^+ \nu_e \bar{\nu}_\mu)} < 1.9 \times 10^{-9}, \quad (2)$$

$$R_{\mu^- + N \rightarrow e^- + N} = \frac{\Gamma(\mu^- + N \rightarrow e^- + N)}{\Gamma(\mu^- + N \rightarrow \nu_\mu + N)} < 1.6 \times 10^{-8}. \quad (3)$$

Recent developments in gauge theories allow finite values for these ratios, usually by postulating the existence of new intermediate leptons.<sup>4</sup> If muon-number nonconservation does occur, the relative values of the ratios (1), (2), and (3) will help distinguish among models.

We report here the results of a new search for the  $\mu^+ \rightarrow e^+ \gamma$  decay carried out at TRIUMF using two large NaI(Tl) crystals. The experiment was performed on the stopped  $\pi/\mu$  channel (M9) with a 100-MeV/c beam composed of 61%  $\pi^+$ , 29%  $\mu^+$ , and 10%  $e^+$ . The setup is shown in Fig. 1. Pions were stopped in a  $15 \times 15 \times 0.6$  cm<sup>3</sup> scintillation-counter target (counter 3) oriented at 20° to the incident beam. The stopping rate was  $2 \times 10^5$ /sec; the decay  $\pi^+ \rightarrow \mu^+ \nu_\mu$  was the source of muons. The

total number of pions stopped during the experiment was  $N_\pi = 3.61 \times 10^{10}$ .

Two NaI(Tl) crystals (TINA, 45.7 cm diam  $\times$  50.8 cm and MINA, 35.5 cm diam  $\times$  35.5 cm)

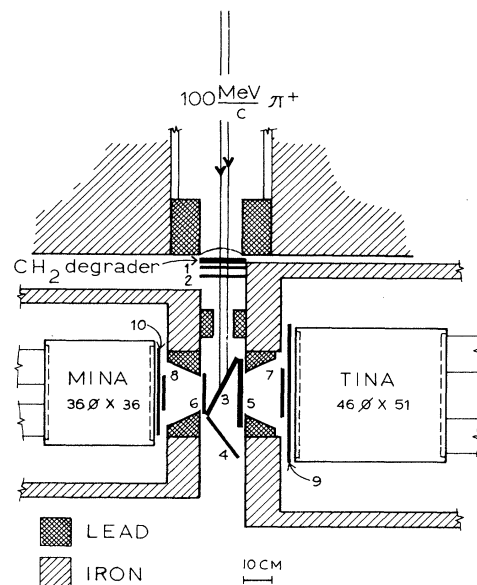


FIG. 1. Diagram of the setup used in the present experiment. The scintillation counters Nos. 1–10 (thickness not to scale) were used to identify charged particles.

viewed the target in close geometry at  $90^\circ$  to the beam direction. Three scintillation counters in front of each crystal detected charged particles originating in the stopping counter with efficiency  $\epsilon_c = (0.99)^3 = 0.97$ . The setup was nearly symmetric for  $e\text{-}\gamma$  (electron in TINA,  $\gamma$  ray in MINA) and  $\gamma\text{-}e$  ( $\gamma$  ray in TINA, electron in MINA) coincidence events. The acceptance for  $e\text{-}\gamma$  and  $\gamma\text{-}e$  events from  $\mu \rightarrow e\gamma$  decay was defined by scintillation counter 8 (12.7 cm diam  $\times$  3.5 mm) and counter 7 (17.8 cm diam  $\times$  3.5 mm) for positrons and by Pb collimators for  $\gamma$  rays. The solid-angle acceptance for  $\mu \rightarrow e\gamma$  events was determined by Monte Carlo simulation<sup>5</sup> to be  $\Omega/4\pi = 0.038$ . The Monte Carlo program was able to reproduce the experimentally measured acceptances for normal- $\mu^+$ -decay positrons (singles events) to within 10%; the acceptance for coincident  $e\text{-}\gamma$  pairs from the radiative<sup>6</sup> decay,  $\mu^+ \rightarrow e^+ \nu_e \bar{\nu}_\mu \gamma$ , with various cuts on the positron or photon energies, was reproduced to within 20%. The total number of radiative-decay events observed with  $E_e > 35$  MeV and  $E_\gamma > 30$  MeV was  $\sim 3000$ .

Neutrons and cosmic-ray backgrounds were reduced by massive iron and concrete shielding. At 50 MeV there were  $\sim 0.05$  counts/MeV/sec in each crystal due to neutrons originating in the region of the pion-production target (located  $\sim 9$  m away). A cosmic-ray anticoincidence shield consisting of ten scintillation counters (1.3 g/cm<sup>2</sup> thick) was placed around each crystal reducing the background from this source to 0.05 counts/MeV/sec in the 50-MeV region.

Data were recorded on-line using a PDP 11/40 computer, interfaced via CAMAC to the electronics. For each  $e\text{-}\gamma$  or  $\gamma\text{-}e$  event, the time differences between the two crystals, the beam counters, and the defining counters 7 and 8 were recorded as well as a sixteen-bit status word describing the scintillation-counter firing pattern which enabled us to perform electron  $\gamma$ -ray discrimination and to reject pileup<sup>7</sup> and beam-related prompt events. In addition, a 10- $\mu$ sec-long pulse vetoed all events following any beam particle that scattered into the counter immediately in front of either crystal. The dead time introduced by these rejections was approximately 3% which produced a trigger efficiency factor,  $\epsilon = 0.97$ .

The energy calibration and resolution for positrons was obtained by fitting the measured positron energy spectrum from normal muon decay  $\mu^+ \rightarrow e^+ \nu_e \bar{\nu}_\mu$  with the  $V-A$  theoretical spectrum folded with the NaI response function. In order to obtain the energy calibration and resolution for

photons the beam polarity was reversed so that the stopped-pion reaction  $\pi^+ + p \rightarrow \pi^0 + n$ ,  $\pi^0 \rightarrow \gamma + \gamma$  could be observed. Although the kinetic energy of the  $\pi^0$ , 2.9 MeV, results in a Doppler-broadened  $\gamma$ -ray spectrum, a 55-MeV line can be obtained in one crystal by requiring the other crystal to have  $E_\gamma^{\text{max}} = 83$  MeV. The crystal resolutions during data taking were 10.5% (10%) full width at half-maximum (FWHM) for positrons and 8.7% (11%) FWHM for photons for TINA (MINA). These values are larger than our previous measurements<sup>8</sup> because of the positron energy loss in the thick stopping counter, the larger acceptance for  $\gamma$  rays, and the higher counting rate used in the present experiment.

Figure 2 shows an  $E_e$  vs  $E_\gamma$  scatter plot of the  $e\text{-}\gamma$  data; Fig. 2(a) includes  $e\text{-}\gamma$  coincidences within the 6.7-nsec (full width) resolving time. Figure 2(b) shows the events in an equivalent accidental background (random  $e\text{-}\gamma$  coincidence) spectrum. The important sources of background which contribute in the region of interest for  $\mu \rightarrow e\gamma$  (50–56 MeV) are summarized in Table I. The most significant background source for this experiment comes from a random coincidence between a positron from normal muon decay,  $\mu^+ \rightarrow e^+ \nu_e \bar{\nu}_\mu$  and a photon from a radiative muon decay,  $\mu^+ \rightarrow e^+ \nu_e \bar{\nu}_\mu \gamma$ . The total number of  $\mu \rightarrow e\gamma$  background events expected for this run was  $b = 1.74$ .

Events in Fig. 2 for which  $E_\gamma > 50$  MeV and  $E_e < 50$  MeV are due to random coincidences between positrons from normal muon decay and neutrons or cosmic rays which escaped detection by the anticoincidence shield. The counts on the high-energy-electron side ( $E_e > 50$  MeV) are due either to  $\pi^+ \rightarrow e^+ \nu_e \gamma$  decay (the event occurred 10 to 100 nsec after a pion stop) or to beam-related events (an incident beam particle which did not stop in counter 3 arrived within  $\pm 100$  nsec of the event).

To confirm the experimental sensitivity at the  $10^{-8}$ – $10^{-9}$  level, we observed simultaneously the rare pion decays  $\pi^+ \rightarrow \pi^0 e^+ \nu_e$  and  $\pi^+ \rightarrow e^+ \nu_e \gamma$  by recording events which occurred  $\sim 15$ – $100$  nsec after a pion stop. In the first case we observed eleven  $\gamma\text{-}\gamma$  events whose energies sum to  $M_{\pi^0}$ . With a calculated geometrical acceptance  $\Omega_{\gamma\gamma}/4\pi = 0.078$ , this corresponds to a  $\pi^0$  branching ratio

$$R_{\pi^0} = \frac{\Gamma(\pi^+ \rightarrow \pi^0 e^+ \nu_e)}{\Gamma(\pi^+ \rightarrow \mu^+ \nu_\mu)} = (0.6 \pm 0.3) \times 10^{-8},$$

compared to the previously<sup>9</sup> measured value,  $R_{\pi^0} = (1.0 \pm 0.08) \times 10^{-8}$ .

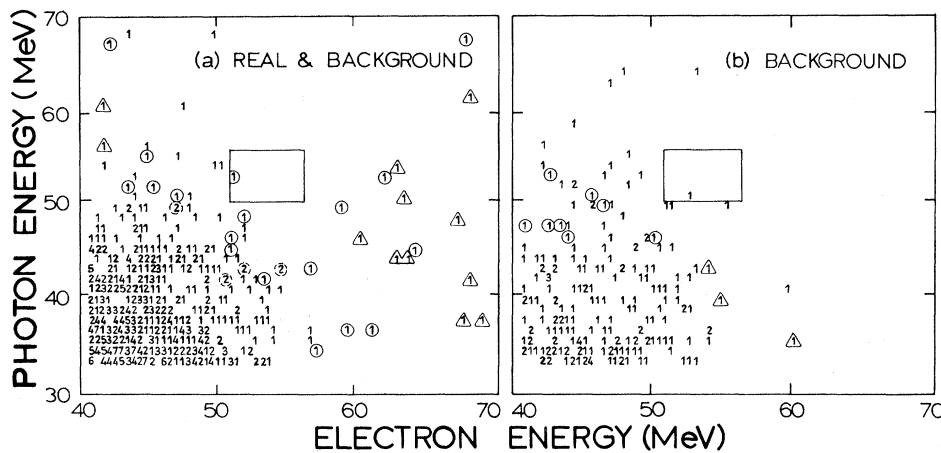


FIG. 2. (a) Energy scatter plot of  $e-\gamma$  data corresponding to a 6.7-nsec window around the peak in the TINA-MINA timing histogram. The numbers shown correspond to the actual number of events observed in the given energy bins  $\sim 0.2 \times 0.2 \text{ MeV}^2$ . The rectangle encloses the region  $(53 \pm 3 \text{ MeV})$  where the  $\mu^+ \rightarrow e^+\gamma$  events are expected. The triangles ( $\Delta$ ) and circles ( $\odot$ ) identify events corresponding to  $\pi^+ \rightarrow e^+\nu_e\gamma$  decay or events associated with the incident beam as described in the text. This identification is shown only in the high-energy region. (b) Scatter plot for random  $e-\gamma$  coincidences occurring in an equivalent time-width window.

In the second case, we observed eight  $e-\gamma$  or  $\gamma-e$  pairs having  $E > 48 \text{ MeV}$ . With a calculated geometrical acceptance  $(\Omega_{e\gamma}/4\pi) + (\Omega_{\gamma e}/4\pi) = 0.029$ , this corresponds to a radiative-pion-decay branching ratio

$$R_\gamma = \frac{\Gamma(\pi^+ \rightarrow e^+\nu_e\gamma)}{\Gamma(\pi^+ \rightarrow \mu^+\nu_\mu)} = (1.6 \pm 0.6) \times 10^{-8},$$

compared to the corrected value of Depommier *et al.*,<sup>10</sup>

$$R_\gamma = (2.15 \pm 0.5) \times 10^{-8}.$$

The solid lines in Fig. 2 enclose the  $E_e-E_\gamma$  (TINA-MINA) region in which  $\epsilon_E = 47\%$  of the events from  $\mu^+ \rightarrow e^+\gamma$  decay would fall.<sup>11</sup> We find one event in the coincidence spectrum [Fig. 2(a)] and one event in the equivalent time-width accidental background spectrum [Fig. 2(b)]. The analysis of the total accidental background region (4 times larger than the real coincidence time window of 6.7 nsec) yields six background events which agrees very well with our calculated background. No events were found for the equivalent  $\gamma-e$  spectra.

TABLE I. Sources of background which can simulate the  $\mu \rightarrow e\gamma$  decay in our apparatus. (A)-(E) are accidental coincidences between a positron from normal muon decay and a second process which either produces or is indistinguishable from a  $\gamma$  ray: (A) A cosmic-ray particle that goes undetected by the anticoincidence shield; (B) a high-energy neutron; (C) a  $\gamma$  ray from radiative muon decay; (D) a positron from normal muon decay that is undetected by the scintillation counters in front of the crystal; and (E) a  $\gamma$  ray from annihilation in the target of a positron from muon decay; (F) is a radiative muon decay in which both the electron and the  $\gamma$  ray are detected. The total expected background is 1.74 events.

Background process	Number of "events" expected during the present experiment
(A) $\mu^+ \rightarrow e^+\nu_e\bar{\nu}_\mu + \text{cosmic ray}$	0.22
(B) $\mu^+ \rightarrow e^+\nu_e\bar{\nu}_\mu + \text{neutron}$	0.24
(C) $\mu^+ \rightarrow e^+\nu_e\bar{\nu}_\mu + \mu^+ \rightarrow e^+\nu_e\bar{\nu}_\mu\gamma$	0.62
(D) $\mu^+ \rightarrow e^+\nu_e\bar{\nu}_\mu + \mu^+ \rightarrow "e^+\nu_e\bar{\nu}_\mu"$	0.21
(E) $\mu^+ \rightarrow e^+\nu_e\bar{\nu}_\mu + \mu^+ \rightarrow e^+\nu_e\bar{\nu}_\mu$	0.39
(F) $\mu^+ \rightarrow e^+\nu_e\bar{\nu}_\mu\gamma$	0.06

To obtain an upper limit on the branching ratio we use the Poisson distribution

$$P_u(n) = (u^n/n!) \exp(-u),$$

where  $u = \epsilon R + b$ ,  $n = 1$  is the observed number of events and,  $b = 1.74$  is the expected number of background events.  $\epsilon$  is the effective number of trials

$$\epsilon = (\Omega/4\pi)\epsilon_c\epsilon_E\epsilon_T N_\pi = 5.96 \times 10^8.$$

At a 90% confidence level<sup>12,13</sup> we find an upper limit for the branching ratio for the  $\mu^+ \rightarrow e^+\gamma$  decay,

$$R_{\mu e \gamma} < 3.6 \times 10^{-9}.$$

We would like to thank the staff at TRIUMF for their help in mounting this experiment. This work was supported in part by the National Research Council of Canada.

<sup>(a)</sup>On sabbatical leave at Physics Department, University of British Columbia, Vancouver, British Columbia V6T 1W5, Canada.

<sup>1</sup>S. Parker, H. Anderson, and C. Rey, Phys. Rev. **133**, B768 (1964).

<sup>2</sup>S. M. Korenchenko *et al.*, Zh. Eksp. Theor. Fiz. **70**, 3 (1976) [Sov. Phys. JETP **43**, 1 (1976)].

<sup>3</sup>D. A. Bryman, M. Blecher, K. Gotow, and R. J. Pow-

ers, Phys. Rev. Lett. **28**, 1469 (1972).

<sup>4</sup>See for example T. P. Cheng and L.-F. Li, Phys. Rev. Lett. **38**, 381 (1977). Also J. D. Bjorken, K. Lane, and S. Weinberg, SLAC Report No. SLAC-PUB-1925 (to be published); their Ref. 2 contains an extensive list of the recent literature on the subject.

<sup>5</sup>G. Opat, Monte Carlo Program, SIMUL 8, TRIUMF Report No. TRI-77-4 (to be published).

<sup>6</sup>G. Källén, in *Springer Tracts in Modern Physics*, edited by G. Höhler (Springer, Berlin, 1968), Vol. 46, p. 96.

<sup>7</sup>Pileup events consisting of two charged particles entering either NaI detector within 400 nsec (twice our integration time for the linear pulses) were detected by the two large plastic counters 9 and 10. Because of the relatively low stopping rate ( $2 \times 10^5 \text{ sec}^{-1}$ ), only 1% of the NaI signals were affected by pileup and therefore this effect contributed only a small broadening of our experimental resolution.

<sup>8</sup>J. Spuller *et al.*, Phys. Lett. **67B**, 479 (1977).

<sup>9</sup>P. Depommier *et al.*, Nucl. Phys. **B4**, 189 (1968).

<sup>10</sup>P. Depommier *et al.*, Phys. Lett. **7**, 285 (1963). The value  $R_\gamma$  quoted has been calculated using the value of  $\gamma$  (ratio of axial-vector to vector form factor) of P. Depommier *et al.* corrected for the latest value of the  $\pi^0$  lifetime [ $\tau_{\pi^0} = (0.828 \pm 0.057) \times 10^{-16} \text{ sec}$ ].

<sup>11</sup>Using the experimentally measure NaI line shape, we estimate that 68% of all particles with incident energy,  $E$ , will deposit an energy in the NaI greater than  $E - 0.5\Delta E$  (FWHM).

<sup>12</sup>Particle Data Group, Rev. Mod. Phys. **48**, 44 (1976).

<sup>13</sup>*Handbook of Mathematical Functions*, edited by M. Abramovitz and I. Stegun (National Bureau of Standards, Washington, D. C., 1964), Vol. 55.

## Whirlpools in the Sea: Polarization of Antiquarks in a Spinning Proton

F. E. Close

Rutherford Laboratory,<sup>(a)</sup> Chilton Didcot, Oxfordshire OX11 0QX, England, and Argonne National Laboratory, Argonne, Illinois 60439

and

Dennis Sivers

Argonne National Laboratory, High Energy Physics Division, Argonne, Illinois 60439

(Received 3 August 1977)

We argue that the sea of virtual quark-antiquark pairs in a proton is polarized. Quantum chromodynamics allows a valence quark to emit a gluon which then produces pairs. If the parent quark in this process exhibits a  $(1-x)^3$  behavior as  $x \rightarrow 1$  then the antiquark with helicity the same as the original quark will have a leading  $(1-x)^5$  distribution. Implications for the counting rules and for polarized Drell-Yan annihilation are discussed.

In our current picture of the proton it contains not only three valence quarks but also an indefinite number of color-SU(3) gauge bosons and quark-antiquark pairs. We usually refer to these extra objects as "gluons" and "the sea", respec-

tively. It is a widely held belief that the sea is unpolarized.<sup>1</sup>

The simplest nucleon configuration consists of just the valence quarks. The sea can be generated by the valence quarks emitting gluons which